A method to identify reproducible subsets of co-activated structures during interictal spikes. Application to intracerebral EEG in temporal lobe epilepsy.

J. BOURIEN, F. BARTOLOMEI*, J.J. BELLANGER, M. GAVARET *, P. CHAUVEL*, F. WENDLING

Laboratoire Traitement du Signal et de L'Image, INSERM

Université de Rennes 1, Campus de Beaulieu, 35042 Rennes Cedex, France.

* Laboratoire de Neurophysiologie et Neuropsychologie, INSERM

Université de la Méditerranée, 13385 Marseille Cedex 5

Published in Clinical Neurophysiology - 2005 Feb;116(2):443-55

Correspondence to:

F. Wendling
Laboratoire Traitement du Signal et de L'Image
Université de Rennes 1 - INSERM
Campus de Beaulieu, Bat. 22
35042 Rennes Cedex - France
Tel : (33) 2 23 23 56 05
fax : (33) 2 23 23 69 17
Email : fabrice.wendling@univ-rennes1.fr

ABSTRACT

Purpose: we present a novel quantitative method to statistically analyze the distribution of multichannel intracerebral interictal spikes (multi-IIS) in stereoelectroencephalographic (SEEG) recordings. The method automatically extracts groups of brain structures conjointly and frequently involved in the generation of interictal activity. These groups are referred to as "subsets of co-activated structures" (SCAS). We applied the method to long duration interictal recordings in patients with mesial temporal lobe epilepsy (MTLE) and analyzed the reproducibility of subsets of structures involved in the generation of multi-IIS for each patient and among patients.

Methods: fifteen patients underwent long-term intracerebral EEG recording (SEEG technique) using depth electrodes. A one-hour period of continuous interictal EEG recording was selected for each patient with precautions regarding the time after anesthesia pre-SEEG, the temporal distance with respect to seizures, the vigilance state of the patient, and the anti-epileptic drug withdrawal. A research of SCAS was conducted on each recording using the developed method that includes three steps: i) automatic detection of monochannel intracerebral interictal spikes (mono-IIS), ii) formation of multi-IIS using a temporal sliding window, iii) extraction of SCAS. In the third step, statistical tests are used to evaluate the frequency of multi-IIS as well as their significance (with respect to the "random distribution of mono-IIS" case).

Results: in each patient, several thousands of multi-IIS (mean±SD, 3322±2190) were formed and several SCAS (mean±SD, 3.80±1.47) were automatically extracted. Results show that reproducible subsets of brain structures are involved in the generation of interictal activity. Although SCAS were found to be variable from one patient to another, some invariant information was pointed up. In all patients, multi-IIS distribute over two distinct groups of structures: mesial structures (15/15) and lateral structures (7/15). Moreover, two particular structures, the internal temporal pole and the temporo-basal cortex, may be conjointly involved with either the first or the second group. Finally, some extracted SCAS seem to match well-defined anatomo-functional circuits of the temporal lobe.

Significance: during interictal activity in MTLE, similar subsets of temporal lobe structures are involved in the generation of spikes. This paper brings statistical evidence for the existence of these subsets and presents a method to automatically extract them from SEEG recordings. Interictal activity is spatially organized in the temporal lobe and preferentially involves two functional systems of the temporal lobe (either mesial or lateral).

Key words: temporal lobe epilepsy, intracerebral EEG, interictal spikes, signal processing, co-occurrence, statistical analysis.

Glossary:

SEEG : StereoElectroEncephaloGraphy

mono-IIS : monochannel Intracerebral Interictal Spike

multi-IIS : multichannel Intracerebral Interictal Spikes

SCAS : Subset of Co-Activated Structures

MTLE : Mesial Temporal Lobe Epilepsy

1. Introduction

During the pre-surgical evaluation of patients suffering from drug-resistant partial temporal lobe epilepsy, intracerebral recordings reflect two types of paroxysmal activity: ictal activity and interictal activity characterized by paroxysmal transient events often referred to as “interictal spikes” when they show a sharp component.

Although the relationship between interictal and ictal activity is an essential and recurrent question in epileptology, it still remains unclear. Nevertheless, the analysis of interictal paroxysmal events is complementary to the analysis of seizures and is recognized as clinically relevant in the study of the organization of the epileptogenic zone.

Numerous works have been dedicated to interictal paroxysmal events for the past decades, both in human (Talairach & Bancaud 1966) and animal models (Avoli & Barbarosie 1999). Penfield and Jasper were the first to study their morphology (Penfield & Jasper 1954). They introduced two classes (primary and propagated) and found that sharper spikes were markers of the epileptogenic lesion. Then a central question was raised about the way to characterize the spatio-temporal distribution of interictal events, both in surface and intracerebral EEG signals (Barth et al 1984, Chauvel et al 1987, Stefan et al 1990). In this latter field, a mapping technique adapted to depth-EEG recording was developed by (Badier & Chauvel 1995) based on the use a high temporal resolution (in the order of the millisecond) to reveal the origin of interictal spikes as well as possible propagation schemes. Several studies based on intracerebral recording in human followed, and also suggested that identification of leading regions implied in interictal activity could help to tailor resections in order to improve seizure control (Alarcon et al 1997) and may be predictive of seizure onset zones (Asano et al 2003, Hufnagel et al 2000).

A common feature of the aforementioned studies is that they always emphasize the importance of characterizing the co-occurrence information. Indeed, this information is crucial for identifying physiopathological systems implied in the generation of transient paroxysmal events that reflects in

EEG signals as multichannel interictal spikes. This problem is particularly complex if one also considers the tremendous amount of spikes (up to several thousands per hour) that can be recorded during a pre-surgical evaluation that usually lasts a few days.

Consequently, from the viewpoint of interictal information processing, we feel the need for quantitative methods able to deal with this co-occurrence information. Such methods are necessary not only to confirm that macroscopic networks are involved in the generation of epileptic interictal activity but also to reveal the general features of such networks from sufficiently large data sets.

The primary purpose of the present study was to describe a novel method for processing long duration SEEG recordings in order to extract subsets (if they exist) of brain structures frequently and conjointly involved in the generation of intracerebral interictal spikes (IIS). In the following, these subsets are referred to as “subsets of co-activated structures” (SCAS). The method proceeds in three steps detailed in section 2.3: i) automatic detection of monochannel intracerebral interictal spikes (mono-IIS), ii) formation of multichannel intracerebral interictal spikes (multi-IIS), iii) automatic extraction of reproducible SCAS using a statistical approach. In the third step, statistical tests are performed to evaluate the significance of extracted sets (“organized spatial distribution of mono-IIS” versus “random spatial distribution of mono-IIS”). The method is aimed at complementing the visual analysis performed by the epileptologist. From SEEG signals, it automatically provides subsets of structures that co-activate during the generation of spikes.

We applied the method in fifteen patients with medically intractable partial epilepsy of temporal origin (mesial temporal lobe epilepsy -MTLE-). Firstly, from simultaneous recording of mesial (hippocampus, amygdala, entorhinal cortex, temporo-basal cortex, internal temporal pole) and lateral (superior, middle and inferior temporal gyri, insula, external temporal pole) structures, the aim was to verify that interictal spikes are spatially organized in the temporal region. Secondly, the objective was to determine subsets of structures that co-activate during the generation of interictal spikes and to relate these subsets to particular anatomo-functional systems in the temporal lobe.

2. Methods

2.1 Patients and SEEG recording

Fifteen patients (6 men, 9 women), aged 14-43 years (mean ± SD, 31.5 ± 8.3) undergoing pre-surgical evaluation of drug-resistant partial epilepsy were selected (numbered from P1 to P15). All patients had a comprehensive evaluation including detailed history and neurological examination, neuropsychological testing, high resolution magnetic resonance imaging (MRI) study, surface electroencephalography (EEG) and stereoelectroencephalography (SEEG, depth electrodes) recording of seizures. The latter was performed during long-term video-EEG monitoring. According to these clinical, anatomical and electrophysiological data, a mesial temporal lobe epilepsy (MTLE) was diagnosed. SEEG was carried out as part of our patients' normal clinical care, and they gave informed consent in the usual way. Patients were informed that their data might be used for research purposes.

We chose to chose to analyze data recorded in patients with MTLE because these patients had intracerebral depth electrodes implanted in well defined brain structures. To select patients, we examined all MTLE cases recorded in the Epilepsy Unit since 1997. We ended with fifteen patients in whom the same brain structures were recorded. Electrodes explored mesial structures (the anterior and posterior part of the hippocampus, amygdala, entorhinal cortex, temporo-basal cortex and internal temporal pole) in addition to lateral sites namely the superior, middle, and inferior temporal gyri, the insula, and external temporal pole. For simplicity, the insula (which lies in the depth of the lateral Sylvian fissure) was put in the group of lateral structures. Table 1 provides clinical information about selected patients. Table 2 provides names and abbreviations for recorded brain structures.

SEEG recordings were performed using intracerebral multiple contact electrodes (10 to 15 contacts, length: 2 mm, diameter: 0.8 mm, 1.5 mm apart) placed intracranially according to Talairach's stereotactic method (Musolino et al 1990, Talairach et al 1974). The positioning of electrodes was determined in each patient based upon available non-invasive information and hypotheses about the localization of the epileptogenic zone. An example of SEEG exploration in the right temporal lobe is presented in figure 1 (patient P6). The implantation accuracy was per-

operatively controlled by telemetric X-ray imaging. A post-operative computerized tomography (CT) scan without contrast was then used to verify both the absence of bleeding and the precise 3D location of each lead. Intracerebral electrodes were then removed and an MRI performed, permitting visualization of the trajectory of each electrode. Finally, CT-scan/MRI data fusion was performed to anatomically locate each contact along the electrode trajectory.

2.2 Data selection

SEEG signals were recorded on a Deltamed™ system with a maximum of 128 channels. They were sampled at 256 Hz and recorded to hard disk (16 bits/sample) using no digital filter. A one-hour period of continuous interictal SEEG recording was selected for each patient except for patients P2 (46 min) and P4 (34 min) in whom analyzed periods were reduced in order to satisfy selection criteria. Short exemplary interictal SEEG segments are displayed in figure 2 (P1) and figure 3 (P3). Some precautions were taken about several factors which are likely to modulate interictal activity (Gotman & Koffler 1989, Gotman & Marciani 1985): i) no recording was selected during the first day of SEEG exploration to avoid possible effects induced by anesthesia performed during surgical procedure of electrode implantation, ii) analyzed period was chosen during daytime and temporally far from seizure periods (one hour, at least), iii) patient was awake (video controlled) and iv) anti-epileptic drug withdrawal was performed three days before at least.

2.3 SEEG signals analysis

2.3.1 Detection of monochannel intracerebral interictal spikes (mono-IIS)

Mono-IIS are generally characterized by a sharp component called spike (or polyspike), sometimes followed by a slow wave (Chatrian et al 1974). A spike is defined as a wave of high amplitude and short duration (“signal”) compared to waves of background EEG (“noise”). The detection of mono-IIS can then be performed by detecting the occurrence of spikes in background EEG. Among possible detection approaches, heuristics methods generally use a first stage for increasing the signal-to-noise ratio and a second stage for deciding whether or not a spike is present.

In the present work, we used a quadratic approach for the first stage (Senhadji et al 1995). At each sample time, the mean value of squared modulus of outputs of a wavelet filter banks is computed. The amplitude of this quantity *q(t)* is random with high mean value during spike or polyspikes duration and low mean value during background EEG. In the second stage, a Page-Hinkley algorithm (Basseville & Nikiforov 1993) was used to automatically estimate time instants corresponding to abrupt changes of *q(t)*. For each patient, detector parameters were adjusted separately from channel to channel by visual inspection of detection times (stored for further analysis) to qualitatively adapt the performances (in terms of false negatives and false positives) of the automatic detection procedure. Indeed using simulations (not reported here), we showed that the entire procedure is more sensitive to false negatives than false positives. This can be easily explained: in the former case, some important information is missed and consequently, this information can not be represented into extracted SCAS whereas in the latter case, false positives generally occur randomly (from channel to channel) and thus do not perturb the formation of SCAS (no co-occurrence). This semi-automatic procedure ensures that relevant information is present at the beginning of the whole procedure of SCAS extraction.

2.3.2 Formation of multichannel intracerebral interictal spikes (multi-IIS)

The purpose of this step is to identify all muti-IIS that include at least 2 co-occurrents mono-IIS in a same temporal interval of duration D. The algorithm proposed in (Bourien et al 2004) was used. Based on the use of a sliding window of duration D, this algorithm builds an $N \times M$ boolean matrix B whose entry b_{ij} is equal to 1 iif one mono-IIS of channel $i \in \{1,...,N\}$ belongs to j^{th} multi-IIS, $j \in \{1,...,M\}$ and b_{ij} is equal to zero otherwise. In the following, matrix B is referred to as the "co-occurrence boolean matrix" (B columns are a summary of co-occurrence information). Experimentally, we obtained good extraction of multi-IIS in MTLE for D values ranging between 100 msec and 250 msec in accordance with range values indicated in (Alarcon et al 1994). D was chosen equal to 150 msec.

2.3.3 Extraction of subsets of co-actived structures (SCAS)

We modelled column vectors B_j of matrix B as M independent realizations of a random vector called $X = [x_1 ... x_N]^*$ (* denoted matrix transposition) whose coordinates are boolean random variables with discrete conjoint probability law P on $\{0,1\}^N$. Let $\{w_1,...,w_n\}$ be an arbitrary subset of n distinct channel indices in $\{1,...,N\}$. The event $\{x_{w_1}=1,...,x_{w_n}=1\}$ will be denoted equivalently $W = \{w_1,...,w_n\}$ and let $P(W)$ be its probability.

The approach proposed to extract SCAS relies on i) the definition of co-concurrency (between IIS observed in co-activated structures) in a probabilistic language and ii) the formulation of statistical criteria for detecting such co-occurrencies.

For i), we will say that spikes observed on the channels whose indices are stored in W are co-occurring if the three following conditions (C1, C2, and C3) are met:

- Minimal probability (C1) : $P(W) \geq \lambda$, $\lambda \in [0,1]$.
- Statistical dependency (C2) :

$$P(W) = P(\{w_n\}/\{w_{n-1},...,w_1\}) \times ... \times P(\{w_2\}/\{w_1\}) \times P(\{w_1\})$$

is such that $P(W) > P(\{w_n\}) \times ... \times P(\{w_1\})$ (1)

- Maximality (C3) : $P(\{w_j\}/W) \leq 1-\eta$, for all $w_j \in \{1,...,N\} - \{w_1,...,w_n\}$, $\eta \in [0,1]$.

Condition C1 allows to select the class CL1 of events W whose probability value is superior to a threshold λ. C2 defines the subclass CL2⊂CL1 for which random variables $\{x_{w_1},...,x_{w_n}\}$ are not mutually independent. Finally, C3 defines subclass CL3, CL3⊂CL2. A subset $W = \{w_1,...,w_n\}$ in CL2 is not included in CL3 if W is not maximal, i.e. conditionnaly to realization of W, there exists at least one additional activated channel w_j, w_j not included in W, with a probability higher than 1-η.

For ii), $P(W)$ are replaced by their estimations $F(W) = \frac{n(W)}{M}$ where $n(W)$ is the occurrence

number of event W and M is the total number of realizations (i.e. number of multi-IIS). Classes CL1, CL2, and CL3 are sequentially obtained as follows:

- An efficient algorithm called APRIORI (Agrawal & Srikant 1994, Mannila et al 1994) is used to extract CL1 from the lattice of all possible subsets (Bourien et al 2004).
- Two confidence intervals I_1 and I_2 (one for each of the two members of inequality (1)) are built such that $P(\log P(W) \in I_1) = P(\sum_{i=1}^{n} \log P(\{w_i\}) \in I_2) = \beta$ and compared to obtain CL2. β denotes the confidence probability. Independence hypothesis is then rejected iif I_1 and I_2 do not intersect (it can be shown that the probability of false positive is overestimated by $2(1-\beta)$). I_1 is classically built under Gaussian approximation of experimental frequency probability law if $M \times F(W)^{\frac{3}{2}} > 1.07$ and $M \times (1-F(W))^{\frac{3}{2}} > 1.07$ (Raff 1956). To built I_2, the law of $\sum_{i=1}^{n} \log P(\{w_i\})$ is also assumed to be Gaussian.
- For each W in CL2, W is put in CL3 iif $F(\{w_j\}/W) = \frac{F(\{w_j, w_1, ..., w_n\})}{F(\{w_1, ..., w_n\})} \leq 1-\eta$ for each $w_j \in \{1, ..., N\} - \{w_1, ..., w_n\}$.

Practically, the checking of these three conditions can be interpreted as a 3-stage-filtering process: the higher parameters λ, β, and η , the more selective the extraction procedure is. Parameter λ sets the minimal frequency of extracted SCAS. It must be chosen according to the above condition (Raff 1956). For example, if M = 200, extracted SCAS become significant for lambda greater than 0.031 (3.1 %). If M=1000, lambda must be greater than 1.2%. Parameter β is the confidence probability in the procedure performed to test the statistical dependency in subset of channels on which events were detected. Finally, parameter η is related to the "autonomy" of a given SCAS. In this study, these parameters were respectively fixed to 0.1, 99.9 % and 0.25 for all analyzed SEEG recordings. According to our personal sensibility parameters λ, β, and η could be selected by the user in the respective ranges [0.01,0.2], [95%, 99.9%], and [0.1,0.25]".

Finally, figure 4 illustrates the three stages of the extraction procedure applied to SEEG signals recorded in P15 (for simplicity, only 5 channels are represented). Detailed information about the three stages described above and about the visualisation of extracted SCAS is provided in the legend of figure 4.

2.3.4 Statistical validation

In order to verify that the three-stages procedure does not keep undesirable SCAS (i.e. sets W with components $x_{w_1},...,x_{w_n}$ independently active) in class CL3, we used Monte-Carlo simulations in which we analyzed mono-IIS with randomly distributed detection times $t_{i,j}$, $0 \le t_{i,j} \le T$ where $i = 1,...,N$ is the channel index, T is the observation duration, $j = 1,...,n_i$ is the index of detected event and n_i is the number of mono-IIS detected on channel i.

These random detection times were simulated according to the probability law of Poisson point processes on $[0,T]$ with rates (i.e. mean number of events by unity of time) $\lambda_i = \frac{n_i}{T}$. The Poisson hypothesis reflects the absence of probabilistic structure (no memory) in the sequence of occurrence times on a given channel. Any other probabilistic model for occurrence times would correspond to the introduction of memory, which is not the case in our problem.

According to interchannel independence hypothesis, generated random processes are mutually independent from channel to channel. A co-occurrence boolean matrix $\tilde{B}$ was obtained by applying the procedure of formation of multi-IIS on simulated processes. Then $\tilde{B}$ was searched for all SCAS actually found in real data and respective frequencies were computed. This procedure was reiterated a large number of times. In theory, the distribution of SCAS frequencies follows a Gaussian distribution (Raff 1956). Its mean ***m*** and standard deviation σ was estimated from experimental distribution. Finally, from ***m*** and σ, we computed the probability value (p-value) corresponding to acceptation of the interchannel independence hypothesis for each SCAS frequency actually computed on real data. Small p-value indicates small probability of extracting a SCAS at given frequency under interchannel independence hypothesis.

3. Results

3.1 Detection of monochannel IIS and formation of multichannel IIS

The detection of mono-IIS was automatically performed on each of the 15 selected SEEG recordings as described in section 2.3.1. To illustrate this step, detected mono-IIS were indicated by asterisks on the two portions of the SEEG recording analyzed in these two patients (figures 2 and 3). The number of detected mono-IIS, presented in table 3, raises two comments. First, the quantity of mono-IIS was found to considerably vary from structure to structure and from patient to patient. The occurrence of mono-IIS is maximal in patient P1 in the internal part of the temporal pole (iTP, 6144 mono-IIS for a one-hour recording) and minimal in patient P2 in the superior temporal gyrus (T1, 1 mono-IIS for a 46-min recording). Second, in patients P1, P6, P7, P8 and P11, a large number of mono-IIS were detected in the lateral structures of the temporal pole (eTP, mT2, T3, aT2, pT2). To synthesize this result, the occurrence rates of mono-IIS per structure were averaged over patients (mean and standard deviations of rows in table 3) and structures were ordered according to this average rate of mono-IIS from the more to the less active. The result, presented in figure 5, shows that mono-IIS occurred more frequently in mesial temporal lobe structures (aH, EC, A, iTP, TbC and pH – descending order) than in lateral temporal lobe structures (T3, aT2, mT2, pT2, T1 – descending order), except for the external part of the temporal pole (eTP).

The formation of multi-IIS from mono-IIS was then performed as described in section 2.3.2. The number of multi-IIS obtained in each patient is given in the last row of table 3. This number is ranging from 7600 (P1) to 492 (P3) (mean±SD, 3322±2190).

3.2 Extraction and representation of subsets of co-activated structures

The whole method was applied to the fifteen recordings of interictal EEG. Fifty seven SCAS were automatically extracted. Results are given in figure 6. They are represented in the same schematic way for the fifteen patients: cerebral structures are positioned along a circle (bottom: mesial temporal lobe, top: lateral temporal lobe) and extracted SCAS are represented using closed contour lines. Surfaces delineated by contours are colored using a grey scale that indicates the SCAS occurrence frequency.

The number of SCAS was found to be variable from patient to patient (n=2 in patients P4, P5 and P12, n=7 in patient P15). However, the analysis of obtained diagrams revealed that SCAS do not randomly distribute in the temporal lobe: subsets were found to be composed of either the structures of the mesial temporal lobe or those of the lateral temporal lobe.

In all patients, at least one SCAS was localized in the mesial temporal lobe. The more frequently encountered SCAS (13/15) is formed by the anterior hippocampus (aH) that co-activates with the entorhinal cortex (EC). In three patients (P1, P6, P8) these two structures co-activate exclusively together. The amygdala was found to be also frequently involved in extracted SCAS (12/15) and, to a lesser extent, the posterior hippocampus (8/15). Moreover, when several SCAS were identified in a given patient, we found that their intersection is never empty and that more frequent SCAS are often included in less frequent ones. This finding means that mono-IIS primarily occur on a subset of several structures and occasionally involve a wider subset of structures. This is, for example, the case for patient P10 in whom spikes mainly involve the subset {aH, EC} and less frequently the subsets {aH, EC, pH}, {aH, EC, iTP} and {A, aH, EC, pH}.

In 7 patients (P1, P6, P7, P8, P11, P14, P15), lateral structures were found to be involved in SCAS. Results show that the external part of the temporal pole (eTP) frequently co-activates with the middle temporal gyrus (T2) and/or the inferior temporal gyrus (T3). We also found that the insula (I) was implied in the SCAS extracted in patients P1 and P6. It also is important to underline that the superior temporal gyrus was found to never co-activate with some other structures.

In 5 patients (P1, P6, P7, P11, P15), some SCAS involving both mesial and lateral structures were identified. Precise analysis of these subsets shows that only two mesial structures may be involved with lateral structures during the generation of interictal activity: the internal part of the temporal pole (iTP) and the temporo-basal cortex (TbC). Indeed, besides these two structures, neither the amygdala nor the hippocampus nor the entorhinal cortex was found to directly co-activate with one of the explored lateral structures. The potential role of the temporal pole and the temporo-basal cortex in the wider propagation of interictal spikes is further discussed.

In summary, we identified three sets of structures conjointly involved in the generation of interictal activity. In the mesial temporal lobe, the first set (referred to as “M1”) includes the amygdala (A),

the hippocampus (aH and pH) and the entorhinal cortex (EC) whereas the second set (referred to as "M2") is composed of the internal part of the temporal pole (iTP) and the temporo-basal cortex (TbC). In the lateral temporal lobe, the third set (referred to as "L") includes the external part of the temporal pole (eTP), the middle and inferior temporal gyrus (T2, T3) and the insula (I).

According to the combination of extracted SCAS over these three sets, we were able to classify the fifteen patients in 6 groups, as summarized in table 4. In the first group (2 patients), extracted SCAS included structures of set M1, only. In the second group (6 patients), SCAS were composed of structures that belonged to sets M1 and M2. In the third group (1 patient), extracted SCAS were found to be formed from structures of sets M1, M2 and L with no intersection between M1/M2 and L. In the fourth group (one patient), SCAS were found in set M1 and in set L, independently. The fifth group (4 patients) correspond to situations (configurations) where SCAS were identified in sets M1, M2 and L with a co-activation of structures belonging to sets M2 and L but no co-activation with those of set M1. Finally, in the sixth group (one patient), SCAS involved some structures of sets M1, M2 and L. In this case, the co-activation of the temporo-basal cortex (TbC) with some structures of set M1 or (exclusive) with some structures of set L was found to occur.

Results show that in seven patients the organization of spikes networks was not limited to mesial structures and so extended beyond the limit of the epileptogenic zone. Indeed, all patients had an epileptogenic zone (defined as the site of primary organization of the ictal discharge) limited to mesial structures (table 5). The temporal lateral structures including the lateral part of the temporal pole were involved only secondarily and with clonic discharge, representing a site of propagation of the ictal discharge. In addition, the difference in the spikes distribution did not seem to influence the post-surgical outcome in these patients (table 5).

3.3.4 Statistical validation

Statistical significance of extracted SCAS was evaluated according to the Monte-Carlo procedure described in section 2.3.4 for each SEEG recording of duration T and for respective n_i values (number of detected spikes per channel) displayed in table 3. Gaussianity of the distribution of SCAS frequency was experimentally verified for 100 simulations for each case. For all SCAS

actually extracted from real data and corresponding frequency, p-value (accept the interchannel independence hypothesis) was always less than 10^{-6}. This result indicates that the probability of finding some SCAS similar to those actually extracted from real data in a process in which occurrence times of mono-IIS would be random is extremely low.

4. Discussion

The principal finding of this study is the following: during interictal activity in MTLE, subsets of temporal lobe structures are conjointly and frequently involved in the generation of spikes. This paper brings statistical evidence for the existence of these subsets and presents a method to automatically extract them from SEEG recordings.

Systems identified in the temporal lobe

In all patients, at least one SCAS was localized in the mesial part of the temporal lobe with a significant incidence of the subset formed by the anterior hippocampus and entorhinal cortex. This result not only confirms the observation made in (Alarcon et al 1997) but is also consistent with respect to available data about hippocampal pathways (axons of the perforant path - major input to the hippocampus - arise principally in layers II and III of the entorhinal cortex which is, in return, an output from the hippocampus).

In 7 patients, some SCAS were identified in the lateral structures of the temporal lobe. This result also confirms frequent observations made from the visual analysis of SEEG recordings regarding the topography of intracerebral spikes: in MTLE, spikes may extend beyond mesial structures in the temporal lobe (Talairach & Bancaud 1966).

Among mesial structures, we observed that the temporobasal cortex and the internal part of the temporal pole can belong to SCAS identified in the mesial temporal lobe as well as SCAS identified in the lateral temporal lobe. We interpret this “pivotal role” mainly by the anatomy of the temporal region (these structures are connected to those of the limbic system and to lateral structures).

More frequent SCAS are always included in less frequent ones. The systems they form are always composed of fewer structures, by definition. A possible interpretation is that these systems may

correspond to primary generators of paroxystic interictal activity which could secondarily drive some other structures, in some cases.

Methodological issues

We showed that reproducible SCAS in the temporal lobe may be extracted among patients. Indeed, TLE is a possible application example. But we also verified that the method is more general: it can be applied in any problem where co-occurrences between transient events recorded on multiple channels are to be statistically characterized. The only condition for application is to be able to assign an occurrence time to each monochannel event. For instance, the method was also applied to the analysis of transient interictal bursts of fast activity (1 second duration in average) in frontal lobe epilepsy (Bourien et al. 2004) where SCAS were also identified.

Conceptually, the proposed method relates to that proposed by Gerstein and collaborators (Gerstein et al 1978) who developed a technique aimed at identifying functionally related neural assemblies and that proposed by Guedes de Oliveira and Lopes da Silva (Guedes de Oliveira & Lopes da Silva 1980) who statistically studied the topography of epileptiform transients in surface epileptic electroencephalograms. It differs from previous works mainly on three points. Firstly, in our method, the step of formation of multichannel events is based on the use of a sliding widow. We showed that is more performant in terms of specificity (through simulations) compared to Gerstein's technique based on fixed duration contiguous windows and Guedes de Oliveira's method in which a window is opened whenever an event is found on one of the analyzed channels.

Secondly, prior to performing statistical tests (conditions C2 and C3), an algorithm (called APRIORI and used in the field of data mining (Agrawal & Srikant 1994, Mannila et al 1994), is used to efficiently select candidate subsets and to avoid the exhaustive test of all possible combinations. Thirdly, the proposed method directly extracts maximal subsets (subsets containing the maximum number of structures for a given frequency) contrary to the two aforementioned methods in which maximality is not tested.

As far as the detection of monochannel events is concerned, we exploited the high frequency component of spike and spike-and-wave complexes. Detection remains a difficult problem considering the variability of spike morphology from structure to structure and from patient to

patient. Nevertheless, we obtained satisfying results on both simulations and real data analyzed by two EEGers and our experience is in accordance with the conclusions of Dumpelmann and Elger (Dumpelmann and Elger, 1999) in which detection problems are dealt with. For concurrent detection methods, readers may also refer to (Alarcon et al 1997, Lieb et al 1978, Lopes da Silva et al 1977) in the field of depth EEG signals or (Frost 1985, Wilson & Emerson 2002) for review in the field of surface EEG signals.

Sequences of detected spikes in extracted SCAS are currently under study. Preliminary results show that sequences might be reproducible (particularly in mesial systems like hippocampus/enthorinal cortex/amygdala) but they might also considerably vary (particularly among neocortical structures).

Clinical interest of the proposed method

This study follows a previous study performed in our group (Badier & Chauvel 1995). At that time, the reproducibility of activation patterns of multi-IIS was already qualitatively observed using spatio-temporal mapping techniques in 13 patients with temporal lobe epilepsy. The present study brings the necessary statistical validation to these observations exploiting the information related to the co-occurrence of mono-IIS.

From the clinical viewpoint, the method can help to improve the diagnostic procedure in patients candidate to surgery. In most epilepsy centers, the topographical analysis of multi-IIS is generally performed visually. The proposed method that automatically builds subsets of structures that are conjointly involved in the generation of interictal spikes can complement visual inspection of long duration EEG recordings. Indeed, although the relationship between interictal and ictal activity still remains unclear, both are recognized as essential signatures (at the EEG level) of underlying epileptic mechanisms. This is attested by the numerous studies dedicated to the analysis of interictal epileptic activity. For instance, in electrocorticography, three studies recently showed that the information contained in time lags of interictal spikes occurring quasi-simultaneously on different channels can be used to better delineate the resection volume in epilepsy surgery (Alarcon et al 1997) or to better localize the « ictal-onset zone » (Asano et al 2003, Hufnagel et al 2000). Precisely, Alarcon and collegues a posteriori studied the origin (leading zone of earliest spikes) and

the propagation (zone of propagated spikes) in multichannel interictal spikes (referred to as "discharges") in electrocorticograms for 42 patients with TLE. In 27 patients, the leading region was included in resection, whereas in the remaining 15 patients, this zone was not removed. Results indicated that in the first group surgical outcome was improved (25/27 seizure free) compared to the second group (4/14 seizure free, one patient did not show spikes).

The second aforementioned study by Hufnagel and collegues dealt with 32 patients with TLE and extra-TLE. Multichannel interictal spikes (called "clusters") were formed using detection and averaging procedure. Then, several parameters are systematically extracted: cerebral zones with earliest spikes in each cluster, maximal average spike amplitude, highest spike frequency and the shortest average spike duration at each recording site. Results showed that some zones were spatially correlated with the ictal-onset zone (especially the ones with earliest spikes). Finally, Asano and collegues' study dealt with 13 children with intractable neocortical epilepsy. Signals showing the highest spike frequency, the highest spike amplitude and the earliest spike in multichannel spikes were found to be frequently included in the set of signals recorded from the ictal-onset zone (respectively 13/13, 12/13, and 10/13).

It is also worthy of note that in most of these studies, no classification is performed on automatically detected multichannel events prior to analysis. In the method proposed in the present work, multichannel events are formed from automatic detection of spikes and a topographic classification is produced in the form of statistically significant subsets of co-activated structures. These subsets can be further interpreted with respect to hypotheses regarding the organization of the epileptogenic zone.

In summary, we have shown that multi-IIS are the reflection of processes involving subsets of temporal structures that co-activate in a reproducible way. Results obtained in 15 patients with MTLE demonstrated that subsets of co-activated structures were localized in the mesial part of the temporal lobe in all patients. In several patients, some subsets were also identified in the lateral structures of the temporal lobe. This led us to categorize patients with respect to mesial and/or lateral structures that are more likely to be conjointly involved in the generation of interictal activity.

Future works

Future works will be oriented towards inline analysis of interictal activity recorded during long-term monitoring with the proposed method and towards the relationship between subsets of structures involved in interictal activity and subsets of structures involved in ictal activity at seizure onset. The proposed method will also allow analysis and better understanding of the organization of interictal activities in all sub-types of temporal lobe epilepsies as well as in extra-temporal epilepsies studied with SEEG. Secondly, this method, particularly its initial step of automatic detection of monochannel intracerebral interictal spikes, can provide objective, quantitative tools helpful for depth analysis of interictal activities. This objective and quantified depth analysis could then be used to evaluate surface interictal spike results provided by source localization tools that still require to be validated by intracerebral data.

References

Agrawal R, Srikant R. 1994. Fast Algorithms for Mining Association Rules. In *Proc. 20th Int. Conf. Very Large Data Bases*, ed. JBBaMJaC Zaniolo, pp. 487: Morgan Kaufmann

Alarcon G, Garcia Seoane JJ, Binnie CD, Martin Miguel MC, Juler J, et al. 1997. Origin and propagation of interictal discharges in the acute electrocorticogram. Implications for pathophysiology and surgical treatment of temporal lobe epilepsy. *Brain* 120 (Pt 12): 2259-82

Alarcon G, Guy CN, Binnie CD, Walker SR, Elwes RD, Polkey CE. 1994. Intracerebral propagation of interictal activity in partial epilepsy: implications for source localisation. *J Neurol Neurosurg Psychiatry* 57: 435-49

Asano E, Muzik O, Shah A, Juhasz C, Chugani DC, et al. 2003. Quantitative interictal subdural EEG analyses in children with neocortical epilepsy. *Epilepsia* 44: 425-34

Avoli M, Barbarosie M. 1999. Interictal-ictal interactions and limbic seizure generation. *Rev Neurol (Paris)* 155: 468-71

Badier JM, Chauvel P. 1995. Spatio-temporal characteristics of paroxysmal interictal events in human temporal lobe epilepsy. *J Physiol Paris* 89: 255-64.

Barth DS, Sutherling W, Engle J, Jr., Beatty J. 1984. Neuromagnetic evidence of spatially distributed sources underlying epileptiform spikes in the human brain. *Science* 223: 293-6

Basseville M, Nikiforov IV. 1993. *Detection of abrupt changes: theory and application*: Prentice-Hall, Inc.

Bourien J, Bellanger JJ, Bartolomei F, Chauvel P, Wendling F. 2004. Mining reproducible activation patterns in epileptic intracerebral EEG signals: application to interictal activity. *IEEE Trans Biomed Eng* 51: 304-15

Chatrian GE, Bergamini L, Dondey M, Klass DW, Lennox-Buctal M, Petersen I. 1974. A glossary of terms most commonly used by clinical electroencephalographers. *Electroencephalogr Clin Neurophysiol* 37: 538-48

Chauvel P, Buser P, Badier JM, Liegeois-Chauvel C, Marquis P, Bancaud J. 1987. The "epileptogenic zone" in humans: representation of intercritical events by spatio-temporal maps. *Rev Neurol* 143: 443-50.

Frost JD, Jr. 1985. Automatic recognition and characterization of epileptiform discharges in the human EEG. *J Clin Neurophysiol* 2: 231-49

Gerstein GL, Perkel DH, Subramanian KN. 1978. Identification of functionally related neural assemblies. *Brain Res* 140: 43-62

Gotman J, Koffler DJ. 1989. Interictal spiking increases after seizures but does not after decrease in medication. *Electroencephalogr Clin Neurophysiol* 72: 7-15

Gotman J, Marciani MG. 1985. Electroencephalographic spiking activity, drug levels, and seizure occurrence in epileptic patients. *Ann Neurol* 17: 597-603

Guedes de Oliveira PH, Lopes da Silva FH. 1980. A topographical display of epileptiform transients based on a statistical approach. *Electroencephalogr Clin Neurophysiol* 48: 710-4.

Hufnagel A, Dumpelmann M, Zentner J, Schijns O, Elger CE. 2000. Clinical relevance of quantified intracranial interictal spike activity in presurgical evaluation of epilepsy. *Epilepsia* 41: 467-78

Lieb JP, Woods SC, Siccardi A, Crandall PH, Walter DO, Leake B. 1978. Quantitative analysis of depth spiking in relation to seizure foci in patients with temporal lobe epilepsy. *Electroencephalogr Clin Neurophysiol* 44: 641-63

Lopes da Silva FH, van Hulten K, Lommen JG, Storm van Leeuwen W, van Veelen CW, Vliegenthart W. 1977. Automatic detection and localization of epileptic foci. *Electroencephalogr Clin Neurophysiol* 43: 1-13

Mannila H, Toivonen H, Verkamo AI. 1994. Efficient algorithms for discovering association rules. In *AAAI Workshop on Knowledge Discovery in Databases (KDD-94)*, ed. UMFaR Uthurusamy, pp. 181. Seattle: AAAI Press

Musolino A, Tournoux P, Missir O, Talairach J. 1990. Methodology of "in vivo" anatomical study and stereo-electroencephalographic exploration in brain surgery for epilepsy. *J Neuroradiol* 17: 67-102

Penfield W, Jasper H. 1954. Epilepsy and functional anatomy of the human brain. *Little, Brown and Company. Boston*

Raff MS. 1956. On approximating the point binomial. *Journal of the american statistical association* 53: 293-303

Senhadji L, Dillenseger JL, Wendling F, Rocha C, Kinie A. 1995. Wavelet analysis of EEG for three-dimensional mapping of epileptic events. *Ann Biomed Eng* 23: 543-52

Stefan H, Schneider S, Abraham-Fuchs K, Bauer J, Feistel H, et al. 1990. Magnetic source localization in focal epilepsy. Multichannel magnetoencephalography correlated with magnetic resonance brain imaging. *Brain* 113 (Pt 5): 1347-59

Talairach J, Bancaud J. 1966. Lesion, "irritative" zone and epileptogenic focus. *Confin Neurol* 27: 91-4

Talairach J, Bancaud J, Szikla G, Bonis A, Geier S, Vedrenne C. 1974. New approach to the neurosurgery of epilepsy. Stereotaxic methodology and therapeutic results. 1. Introduction and history. *Neurochirurgie* 20: 1-240.

Wilson SB, Emerson R. 2002. Spike detection: a review and comparison of algorithms. *Clin Neurophysiol* 113: 1873-81

Patients	Gender/ Age	Historical findings	Type of epilepsy	MRI abnormalities
P1	F/43	FS at 8 mo (encephalitis)	L-MTLE	Bilateral HS Left > Right
P2	F/31	-	R-MTLE	Normal
P3	M/28	FS at 6 y	L-MTLE	Left HS
P4	F/14	FS at 10 mo	L-MTLE	Left HS
P5	F/43	FS at 1 y	R-MTLE	Right HS
P6	M/30	FS at 15 mo	R-MTLE	Right HS Left frontal arachnoidian cyst
P7	F/31	FS at 2 y	L-MTLE	Left HS
P8	F/30	Encephalitis at age 7	L-MTLE	Left HS
P9	M/34	-	L-MTLE	Normal
P10	F/29	-	R-MTLE	Right HS
P11	M/15	-	L-MTLE	Left HS
P12	M/36	FS at 1-3 y	L-MTLE	Left HS
P13	F/35	FS at 11 mo	R-MTLE	Right HS
P14	F/38	FS from 1 to 2 y Familial history of epilepsy	L-MTLE	Bilateral HS Left > Right
P15	M/35	-	L-MTLE	Normal

Table 1. Patient data. M: male, F: female, FS: febrile seizure; R-MTLE: right mesial temporal lobe epilepsy; L-MTLE: left mesial temporal lobe epilepsy, HS: MRI suggestive of hippocampal sclerosis (atrophy and hyperintensity on T2 sequences), mo: month, y: year.

	Cerebral structures	Abbreviation
Mesial	amygdala	A
	anterior hippocampus	aH
	entorhinal cortex	EC
	posterior hippocampus	pH
	temporobasal cortex	TbC
	internal temporal pole (*)	iTP
Lateral	middle part of inferior temporal gyrus	T3
	posterior part of middle temporal gyrus	pT2
	middle part of middle temporal gyrus	mT2
	anterior part of middle temporal gyrus	aT2
	superior temporal gyrus (**)	T1
	insula (**)	I
	external temporal pole (*)	eTP

Table 2. Names and abbreviations of mesial and lateral structures explored with stereoelectroencephalography (SEEG). T1, T2, and T3 respectively indicate superior, middle and inferior temporal gyrus. (*) Not explored in P5. (**) Not explored in P14 and P15. Note that for simplicity, insula was added in the group of lateral structures.

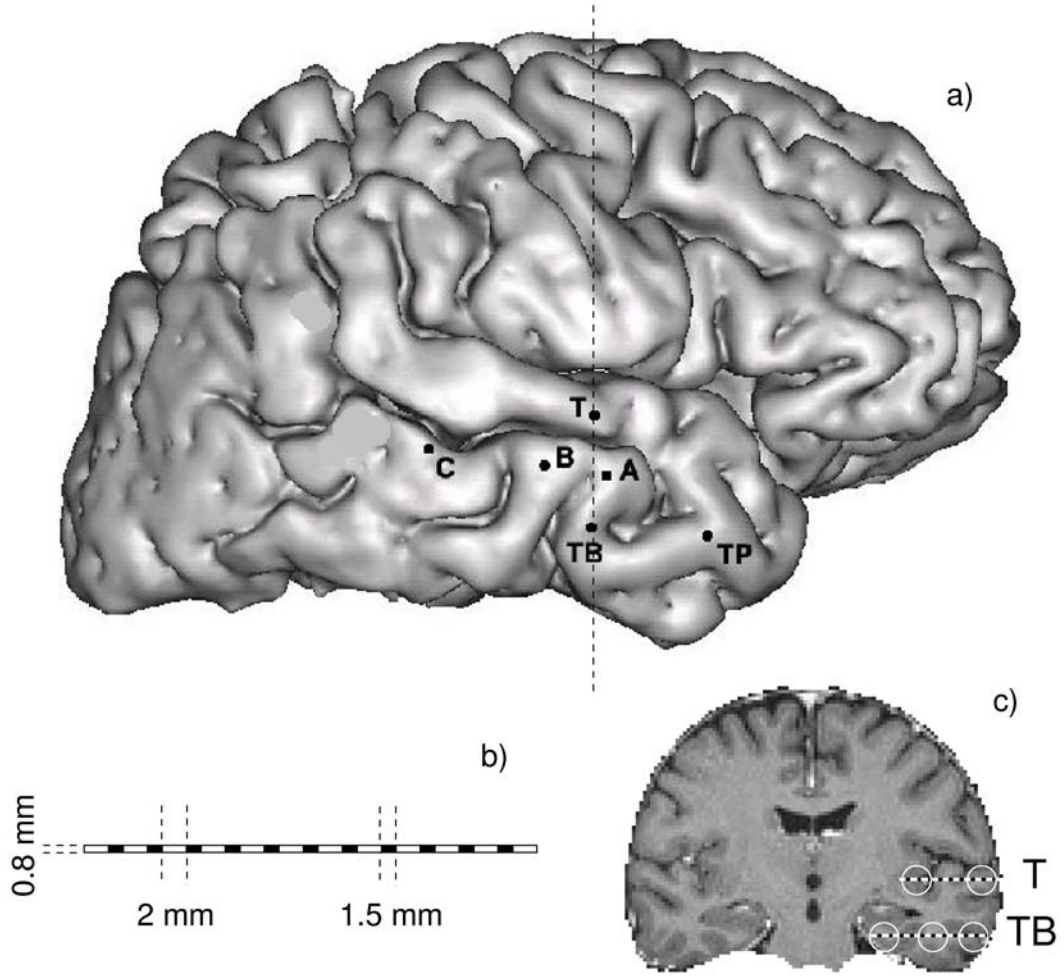

Figure 1. Example of depth electrodes implantation for SEEG in temporal lobe epilepsy. a) Lateral view of all depth electrodes (patient P6) superimposed on a 3D image. 13 structures (6 in mesial TL and 7 in lateral TL) are explored with six intracerebral multiple contact electrodes denoted by letters A, B, C, TP, TB, T. Internal contacts of electrodes TP, A, B, and C record 4 mesial structures (resp. internal temporal pole, amygdala, anterior hippocampus, and posterior hippocampus) while external contacts record 4 lateral structures (resp. external temporal pole, anterior part of middle temporal gyrus -T2-, middle part of T2, posterior part of T2). Internal and external contacts of electrode T explore 2 lateral structures (resp. insula and superior temporal gyrus). Internal and median contacts of electrode TB explore 2 mesial structures (resp. entorhinal cortex and temporobasal cortex) while external contacts explores one lateral structure (inferior temporal gyrus). b) Dimensions of an intracerebral electrode with 12 contacts (white rectangles). c)

Coronal view of the pre-operative plan defined by parallel electrodes T and TB. Location of insula and superior temporal gyrus (recorded by electrode T) and entorhinal cortex, temporobasal cortex and inferior temporal gyrus (recorded by electrode TB) are indicated with white circles. Monopolar SEEG signals were recorded with respect to a reference lead located in the skull.

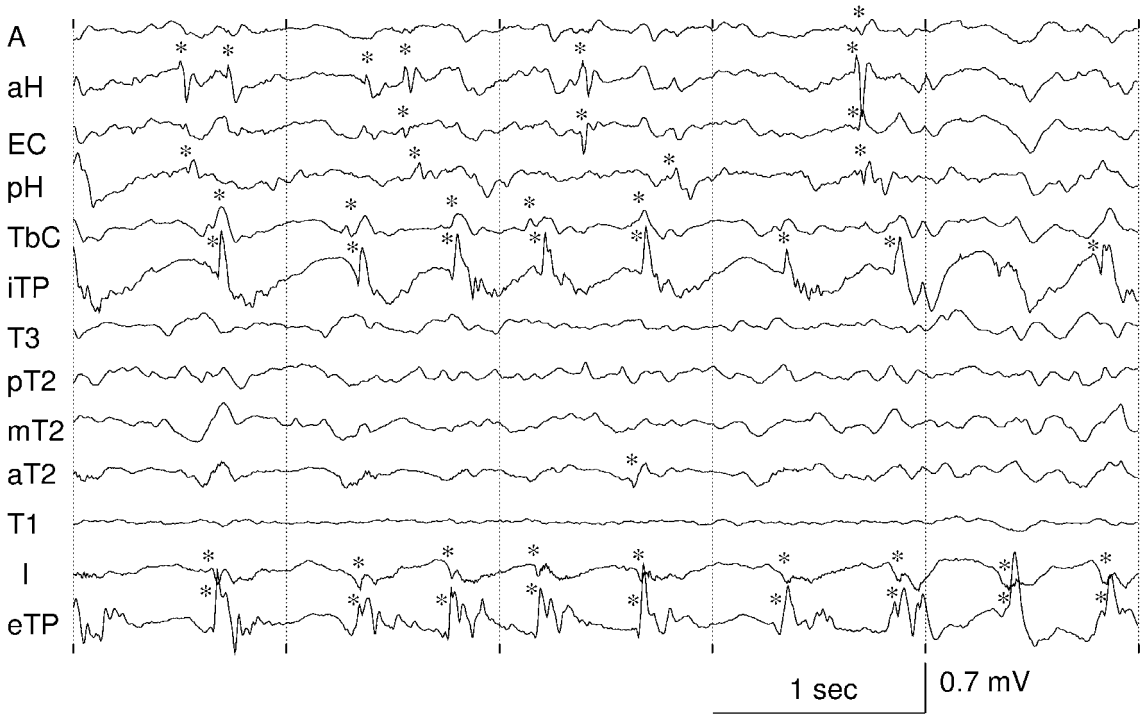

Figure 2. A first example of interictal SEEG recording (5 second duration, patient P1). Asterisks indicate automatically detected mono-IIS. From visual inspection, one can notice that the frequency of multi-IIS is high (approximately 12 multi-IIS in the displayed portion). A frequent co-occurrence of spikes is observed on subset {aH, EC} on the one hand and on subset {I, eTP, iTP}, on the other hand.

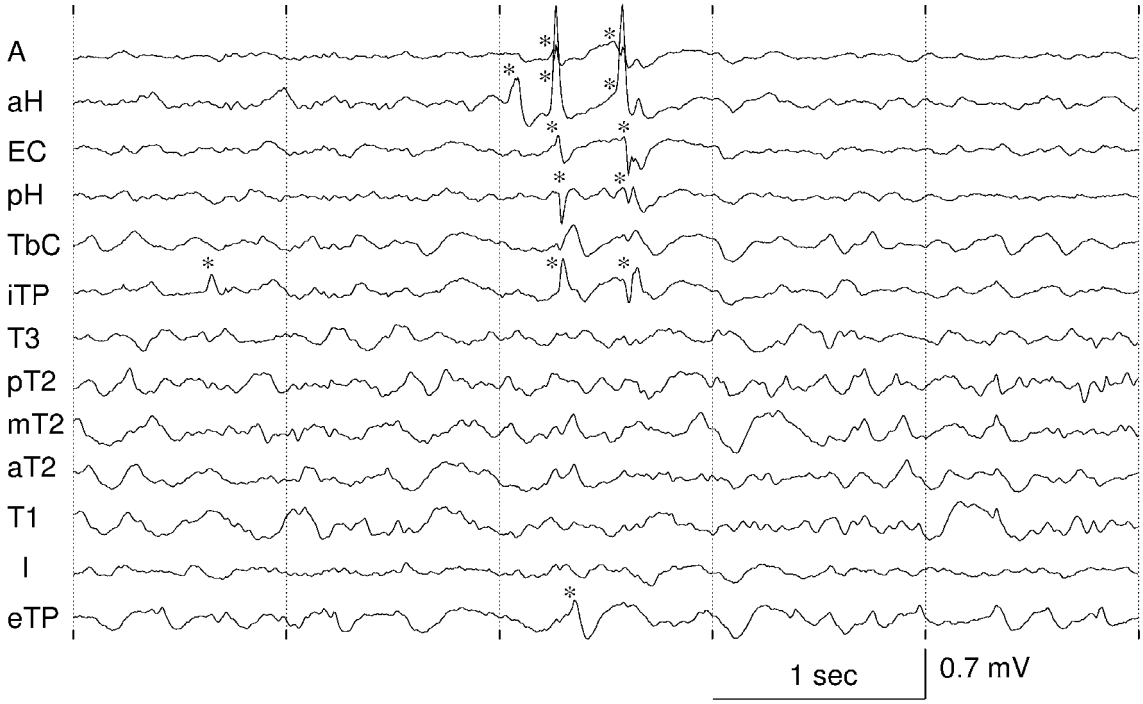

Figure 3. A second example of interictal SEEG recording (5 second duration, patient P3). Asterisks indicate automatically detected mono-IIS. Here, the frequency of multi-IIS is lower than in the example of figure 2 (2 multi-IIS for the 5 displayed seconds). Five mesial structures (amygdala, anterior hippocampus, entorhinal cortex, posterior hippocampus and temporal pole) seem to be conjointly involved in interictal activity.

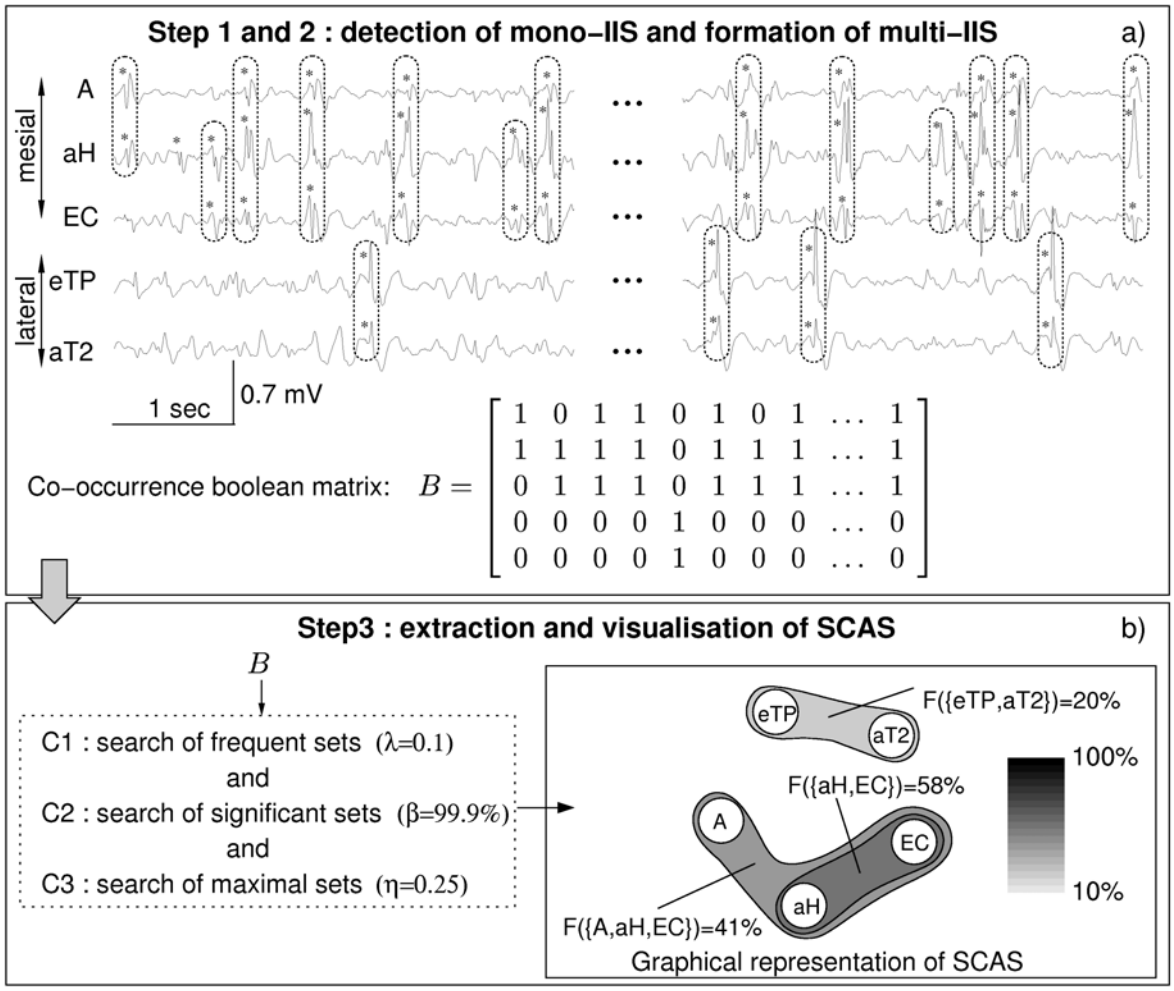

Figure 4. Proposed method for automatic extraction of SCAS and display. This example is reduced to 5 temporal lobe structures for simplicity. The method is applied to vectorial SEEG signal and proceeds in three steps: a) in step 1, mono-IIS are automatically detected (occurrence times are pointed out using asterisks). In step 2, multi-IIS (at least involving 2 mono-IIS distant of less than 150 msec) are automatically formed (rectangles in dotted line). At this stage, the co-occurrence boolean matrix B is built such that entry b_{ij} is equal to 1 if a mono-IIS in channel i is present in the jth multi-IIS and is equal to 0 otherwise. For exemple, in the first multi-IIS, a spike was detected on the first (A) and the second channel (aH). The corresponding multi-IIS is coded as vector $\left[1\,1\,0\,0\,0\right]^{*}$ (* denoted matrix transposition). In step 3, the research of SCAS is performed. For parameter setting λ=0.1, β=99.9%, and η=0.25, three SCAS {aH,EC}, {A,aH,EC} and {eTP,aT2} of respective frequency 0.58, 0.41, et 0.2 are automatically extracted and displayed using closed contours. Grey level indicates occurrence frequency.

		P1	P2	P3	P4	P5	P6	P7	P8	P9	P10	P11	P12	P13	P14	P15
Mesial	**A**	441	1454	280	893	286	1467	2332	395	1092	1477	1101	5636	2008	2291	3639
	aH	2077	489	823	885	304	1930	2929	1082	938	1568	1498	2601	3065	6363	4541
	EC	1637	1086	350	847	310	1356	2429	1167	1464	993	363	5235	2389	2905	3675
	pH	1037	772	252	765	622	918	1696	161	937	915	628	1371	655	1377	3038
	TbC	4580	195	224	49	410	1668	3106	1384	850	550	523	414	720	1506	3400
	iTP	6144	1245	271	583	NE	3505	1596	747	1843	569	1741	709	546	1151	2646
Lateral	**T3**	350	165	89	26	429	2161	2091	1794	360	183	307	211	108	1459	1852
	pT2	304	317	113	23	156	618	293	1460	483	78	1026	59	213	642	47
	mT2	152	151	35	22	42	379	2503	2028	578	187	37	181	95	862	865
	aT2	1423	173	73	75	17	710	2030	1487	681	544	1056	538	29	796	2058
	T1	284	56	18	12	45	491	77	79	52	107	16	14	30	NE	NE
	I	4922	1	57	163	3	2276	1192	36	84	345	43	10	272	NE	NE
	eTP	6071	219	244	60	NE	2571	1400	2669	674	186	783	432	510	937	3631
Number of multi-IIS		**7600**	**1737**	**492**	**1026**	**435**	**4900**	**4552**	**3073**	**2542**	**1760**	**2210**	**5278**	**2707**	**5406**	**6121**

Table 3. Number of detected mono-IIS per brain structure for the 15 analyzed recordings.

Recording duration was equal to 1 hour, except in patient P2 (46 min) and patient P4 (34 min).

NE : not explored.

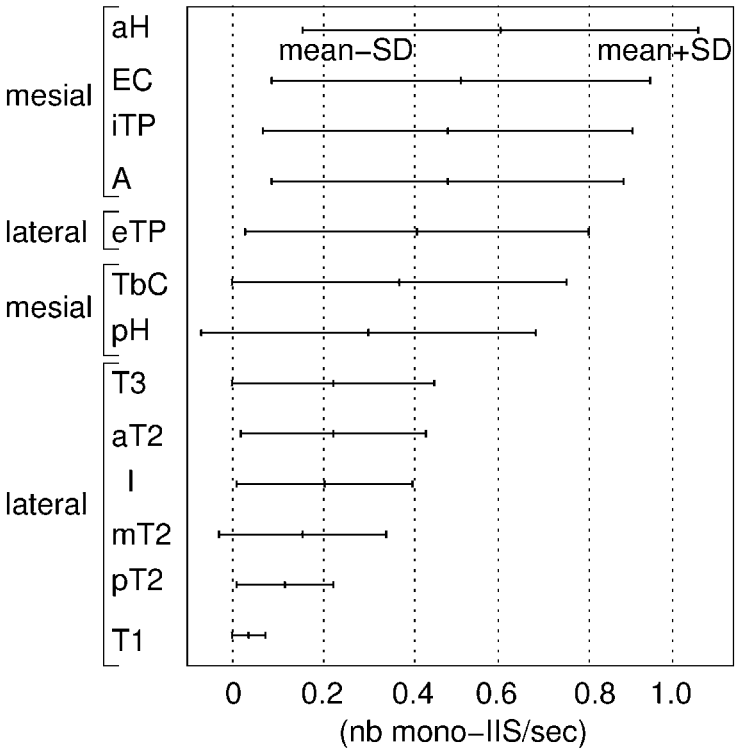

Figure 5. Mean and standard deviation of occurrence rates of mono-IIS for each of the 13 brain structures explored in the 15 studied patients. Structures are ordered from most active (highest spike occurrence rate) to less active (lowest occurrence rate). The anterior hippocampus exhibits a maximal average rate of 0.6 mono-IIS/sec. The high standard deviation measured in all structures indicates strong variability from patient to patient.

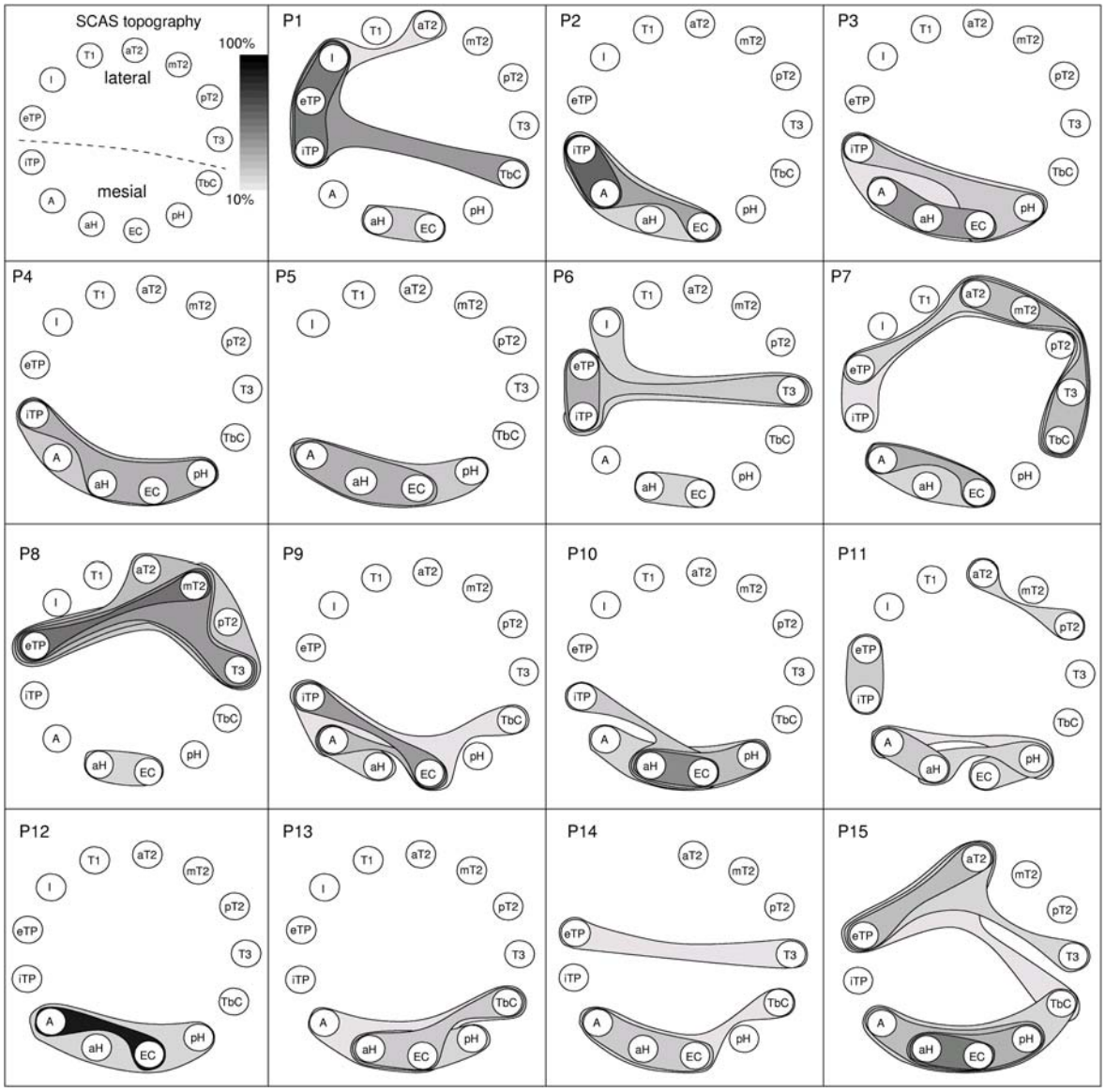

Figure 6. Topographic display of extracted subsets of co-activated structures (SCAS) in the 15 studied patients. A schematic representation is used in which the 13 explored structures are positioned over a circle (upper half circle: lateral structures of the temporal lobe, lower half circle: lower structures of the temporal lobe). SCAS are denoted by closed contours. Grey level indicates occurrence frequency (grey scale in upper left box, quantification step of 5%).

		M1 (A, aH, EC, pH)	**M2 (TbC, iTP)**	**Lateral (T3, pT2, mT2, aT2, T1, I, eTP)**
1	P5, P12	All		
2	P2	A, aH,EC	iTP	
	P3, P4, P10	All	iTP	
	P9	A, aH,EC	TbC,iTP	
	P13	All	TbC	
3	P14	A, aH, EC	TbC	T3, eTP
4	P8	aH,EC		T3,pT2,mT2,aT2, eTP
5	P1	aH, EC	TbC,iTP	aT2, I, eTP
	P6	aH, EC	iTP	T3, I, eTP
	P7	A,aH,EC	TbC,iTP	T3, mT2, aT2, eTP
	P11	All	iTP	eTP
6	P15	All	TbC	T3, aT2, eTP

Table 4. Classification of the 15 patients according to the topography of identified SCAS. The 13 explored structures are partitioned in three groups referred to as M1 (A, aH, EC, pH), M2 (TbC, iTP), and L (T3, pT2, mT2, aT2, T1, I, eTP). The distribution of SCAS over the three groups M1, M2, and L is indicated by thick line rectangles. For exemple, in patient P14, SCAS include three structures of group M1 (A, aH, EC) and one structure of group M2 (TbC) on the one hand and two structures of group L (T3, eTP) on the other hand (no intersection between M1/M2 and L). Note that in patient P15, a structure of group M2 (TbC) co-activates with both all structures of group M1 and three structures of group L (T3, aT2, eTP). This particular behavior of structure TbC is indicated by dotted lines.

Patient	L networks	M networks	Seizure Onset zone (EZ)	Postoperative Engel Class
P1	+	+	M	IA
P2	-	+	M	III
P3	-	+	M	IA
P4	-	+	M	IA
P5	-	+	M	IB
P6	+	+	M	IA
P7	+	+	M	IIA
P8	+	+	M	IA
P9	-	+	M	IA
P10	-	+	M	IA
P11	+	+	M	IIA
P12	-	+	M	IA
P13	-	+	M	IIA
P14	+	-	M	IA
P15	+	+	M	NO

Table 5. Topography (mesial/lateral) of extracted SCAS, seizure onset zone and surgical outcome. L: lateral SCAS, M: mesial SCAS, EZ: epileptogenic zone, M: seizure onset in mesial structures, NO: not operated